



Polysaccharides from *Athyrium multidentatum* (Doll.) Ching an Attenuated D-Galactose-Induced Mouse Aging via SIRT1-p53-p21 Pathway

Jie Mu¹, Dongmei Liu^{1*}, Jiwen Sheng¹, Zhijian Li¹, Weifen Zhang¹, Shumei Mao¹, Liang Jing¹, Jingru Jiang¹ and Li Qi²

¹Department of Pharmacy, Weifang Medical University, Weifang, PR China

² Clinical College of Medicine, Weifang, PR China

ABSTRACT

In this paper, the anti-aging effect of polysaccharides from *Athyrium multidentatum* (Doll.) Ching (AMC) and the underlying mechanisms was investigated employing D-galactose (D-gal) induced aging mouse model. Cytokine levels were detected by enzyme-linked immunosorbent assay (ELISA). Antioxidant enzyme activity and lipid peroxide content were determined by ultraviolet-visible spectrophotometry. Real-time quantitative reverse transcription polymerase chain reaction (qRT-PCR) and western blot assays were performed to assess the genes and proteins expression. Our results suggested that AMC polysaccharides strikingly ameliorated the pathological changes in hippocampus, adjusted the organ indices, increased the serum interleukin-2 (IL-2) content, and decreased the tumor necrosis factor- α (TNF- α) and malondialdehyde (MDA) levels. Furthermore, AMC polysaccharides notably augmented superoxide dismutase (SOD)/catalase (CAT) activities and silent information regulator 1 (SIRT1) gene expression, and lowered p53/p21 mRNA and p53 protein levels. Available data obtained with in vivo model suggested that AMC polysaccharides did display marked anti-aging activity. The mechanisms might attribute to their capacities of augmenting antioxidant enzyme activities, improving immunity function, suppressing lipid peroxidation reaction and regulating SIRT1/p53/p21 signaling pathway.

Keywords: Aging; *Athyrium multidentatum* (Doll.) Ching; D-galactose; Polysaccharides; SIRT1/p53/p21 signaling pathway

INTRODUCTION

Athyrium multidentatum (Doll.) Ching (AMC) is a promising pteridophyte flora with the medicinal values of preventing and curing high blood pressure, parasite and rheumatism diseases. Many active constituents have been found from AMC such as polysaccharides, striatisporolide A, physcion and so on [1,2]. Bioactivity evaluation results suggested that polysaccharides from AMC possessed powerful antioxidative and anti-aging capacities [3-5]. However, the exact anti-aging mechanism is far from being fully elucidated.

Aging can be induced by various cellular stressors, including telomere erosion, DNA damage, oxidative stress or oncogenic activation, which may lead to age-related diseases such as atherosclerosis, osteoporosis, renal failure, Alzheimer's and Parkinson's diseases [6]. Multiple signaling pathways are involved in the process, such as SIRT1-p53-p21 pathway. Oxidative stress-induced p53-dependent DNA damage responses may trigger cell cycle arrest via p53/p21 or p16/pRb pathways and evoke cellular senescence [7-9]. SIRT1 is a pivotal negative regulator of p53-mediated pathways by modulating the acetylation status and transactivation activity of p53 [10]. Doan et al. reported that Yulansan polysaccharides exhibited anti-aging effect in mice through decreasing p53 and p21 genes expression [11]. Furthermore, senescence-associated secretory phenotype (SASP), one of the significant hallmarks

of senescent cells, has an affinity with aging and age-related disease. For instance, proinflammatory cytokine TNF- α can initiate inflammation and senescence.

However, little is known about whether SIRT1/p53/p21 pathway or certain SASP is involved in the anti-aging mechanisms of AMC polysaccharides. In this study, a series of experiments were conducted to investigate the anti-aging effect of AMC polysaccharides and the probable mechanisms by D-gal-induced aging mouse model.

EXPERIMENTAL SECTION

Materials

Athyrium multidentatum (Doll.) Ching rhizome was harvested in Changbai Mountain area of China and stored in a dry and ventilated room. Vitamin E and D-gal were purchased from Sigma Chemical Co., Ltd. (St. Louis, MO, USA). SOD, CAT and BCA protein assay kits were obtained from Beyotime Biotechnology Co., Ltd. (Shanghai, China). Mouse IL-2 and TNF- α ELISA kits were from MultiSciences (Lianke) Biotech. Co., Ltd. (Hangzhou, China). Omega R6934-01 total RNA kit II was procured from Beijing winter song Boye Biotechnology Co., Ltd. (Beijing, China). HiFiScript gDNA removal cDNA synthesis kit was from Beijing ComWin Biotech Co., Ltd. (Beijing, China). SYBR® green realtime PCR master mix was purchased from Toyobo Co., Ltd. (Osaka, Japan). SIRT1, p53, p21 and β -actin primers were synthesized by Sangon Biotech. Co., Ltd. (Shanghai, China). p53 and β -actin polyclonal antibody (rabbit anti-mouse, 10442-1-AP and 20536-1-AP), and peroxidase-conjugated affinity pure goat anti-rabbit IgG (H+L) antibody (SA00001-2) were obtained from Proteintech Group (Rosemont, USA). SuperSignal® West Pico ECL chemiluminescent substrate was purchased from Pierce Biotechnology (Rockford, USA).

Preparation of AMC Polysaccharides

2 kg powdered AMC rhizome was refluxed in distilled water for 1.5 h twice. The extract was concentrated to approximately 200 mL and then added 600 ml anhydrous ethanol. The resultant precipitation was gathered by filtration through a Buchner funnel and 45.6 g of AMC polysaccharides were obtained.

Essential Oil Extraction

Dried material was subjected to hydrodistillation (250g of each sample in 3 L of distilled water) using a modified Clevenger type apparatus for 3h. The essential oil were dried over anhydrous sodium sulfate and stored in the dark.

Animals and Experimental Protocol

A total of eighty male Kun Ming mice, weighing 40 ± 2 g, were obtained from Experimental Animal Center of Shandong Province, Jinan, China (Certificate No. SCXK 20140007). The mice were housed in an environmentally controlled room under a 12 h light/dark cycle at $25 \pm 1^\circ\text{C}$ with free access to food and water throughout the whole study. All experiments were approved by the ethics committee of Weifang Medical University and all efforts were made to minimize animal suffering. The mice were acclimatized for three days, then randomly divided into six groups: normal group (NG), positive control group (VE), model group (DG), low-dose polysaccharide group (LG), medium-dose polysaccharide group (MG) and high-dose polysaccharide group (HG). Except for the normal group, other five groups were intraperitoneal injected with D-gal at 100 mg/kg per day to establish aging model. Meanwhile, vitamin E (25 mg/kg) and polysaccharides (100, 200, and 400 mg/kg) suspended in 0.5% sodium carboxymethyl cellulose (CMC) were orally administered for 50 consecutive days. Normal saline was administered to mice in the normal and model groups, accordingly. The dosage was adjusted according to the mouse daily weigh.

All mice were sacrificed at the end of treatment. Blood samples were collected from the eyes and centrifuged at 3000 r/min for 10 min at 4°C. Serum samples were obtained and stored at -20°C. The brains were fixed in 4% paraformaldehyde solution and stained with hematoxylin and eosin (HE) to observe the pathological changes in hippocampal tissue. The hearts, spleens and livers were weighted after removing the blood. The organ index was calculated as organ weight (mg)/body weight (g). Afterwards, some livers were preserved in liquid nitrogen for qRT-PCR and western blot assays. Other livers were grinded in normal saline and centrifuged at 3000 r/min for 10 min at 4°C. The resultant supernatants were collected and stored at -20°C for enzyme activity assays.

Biochemical Analysis

The levels of IL-2 and TNF- α were measured by ELISA method. SOD/CAT activities and MDA content were determined by ultraviolet-visible spectrophotometry. Protein content was measured by BCA protein assay kit. All operations were performed on a microplate spectrophotometer (Bio-Tek, USA) according to the manufacturer's instructions.

qRT-PCR Analysis

Total RNA was isolated from the liver tissue using Omega R6934-01 total RNA kit II and following the manufacturer's protocol. RNA quality was checked by measuring the optical density ratio at 260/280 nm on a biophotometer plus spectrophotometer (Eppendorf, German). Total RNA (1 μ g) from each sample was reverse transcribed into cDNA. The following oligonucleotides were used to detect the expression levels of the genes: 5'-TAC AAG AAG TCA CAG CAC AT-3' and 3'-GAT AGG TCG GCG GTT CAT-5' primers for p53; 5'-AGC AGA TTA AGC ACA TCC T-3' and 3'-CTC CAT CTC TAA GCC ATC C-5' primers for p21; 5'-GAC TCT TCT GTG ATT GCT AC-3' and 3'-CGC TTA CTA ATC TGC TCC T-5' primers for SIRT1; 5'-ATA TCG CTG CGC TGG TCG TC-3' and 3'-AGG ATG GCG TGA GGG AGA GC-5' primers for β -actin. The PCR protocol was consisted of the following steps: 95°C for 60 s, 40 cycles at 95°C for 15 s, 60°C for 60 s and 72°C for 45 s, and performed on a Lightcycler 480 II PCR instrument (Roche).

Western Blotting Analysis

A total of 30 mg mouse liver was extracted with RIPA lysis buffer and the protein concentrations were determined by the standard BCA method according to the manufacturer's protocol. 30 μ g of protein from each group was subjected to SDS-PAGE electrophoresis (10% separating gel and 5% stacking gel) at 100 V for 1 h and electroblotted onto 0.22 μ m PVDF membrane at 250 mA for 1 h in an ice bath. Membrane was incubated overnight at 4°C with the specific primary antibodies labeled rabbit anti-mouse used to direct against p53 and β -actin at dilutions of 1:1000 and 1:2000 after the membrane was blocked in 5% milk for 2 h. Afterwards, the membrane was rinsed three times with buffer and incubated with second antibody labeled goat anti-rabbit IgG at a dilution rate of 1:3000 for 2 h at room temperature. After the membrane was rinsed three times with buffer again, the immunobands were visualized with a chemiluminescent substrate solution after 5 min of reaction and exposed to the x-ray films for 30 s. The data were obtained and analyzed using the Photoshop software (Adobe Photoshop CS5, USA) and normalized against β -actin.

Statistical Analysis

All data were expressed as mean values \pm standard deviation (SD). Data were statistically analysed using the statistical software of Microsoft Excel 2003. A two-tailed paired t-test was performed for comparison between groups. Statistical significance was considered when $P < 0.05$.

RESULTS AND DISCUSSION

Mouse Hippocampal Slice and Organ Index

Pathological changes in the hippocampal tissues were observed after administering D-gal for 50 consecutive days. Cells in sector CA1 of the cornu ammonis (CA, Ammon's horn) was recorded in Figure 1. Compared with the normal group, cells in the model group were atrophied and maldistributed with blurred boundary, the cell number significantly lessened and the cellular apoptosis was observed. These results meant that the aging mouse model induced by D-gal was successfully established. As shown in Figure 1 D, the pathological changes in CA1 sectors were ameliorated after treatment with AMC polysaccharides.

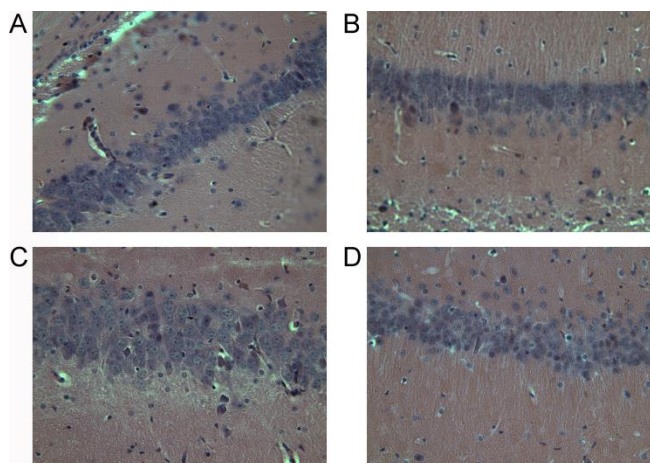


Figure 1. Effect of AMC polysaccharides on mouse hippocampus tissue. Optical images at 40 x magnification of area CA1 of the mouse hippocampal slices. A) presents normal group. B) presents model group. C) presents positive control group. D) presents polysaccharide group

Moreover, AMC polysaccharides strikingly minimized the deteriorious effects of D-gal through increasing the heart/spleen indices and abating the liver index. As shown in Table 1, the heart index in the low- and high-dose polysaccharide groups was higher than the positive control group. However, the liver index in the two groups was lower than the positive control group. The spleen index in the medium- and high-dose polysaccharide groups was beyond the positive control group.

Table 1. Effect of AMC polysaccharides on organ index in aging mouse induced by D-gal (n = 8)

Groups	Heart index (mg/g)	Spleen index (mg/g)	Liver index (mg/g)
NG	6.6 \pm 0.58	3.26 \pm 0.45	46.8 \pm 3.3

DG	5.45±0.73*	2.94±0.36	47.03±2.27
VE	5.61±0.65**	3.06±0.58	43.72±2.6* ^Δ
LG	6.32±0.75 ^Δ	2.99±0.73	42.48±2.69* ^Δ
MG	5.56±0.38**	3.38±0.93	43.78±4.37
HG	6.25±1.09	3.36±0.86	42.79±1.98* ^{ΔΔ}

Note: * $P < 0.05$, ** $P < 0.01$, compared with the normal group (NG). ^Δ $P < 0.05$, ^{ΔΔ} $P < 0.01$, compared with the model group (DG).

Effect of AMC Polysaccharides on IL-2 and TNF- α Contents

Figures 2 and 3 displayed the levels of TNF- α and IL-2 in aging mice serum. Compared with the normal group, IL-2 level was reduced and TNF- α content was raised after D-gal treatment. The level of IL-2 in the low-dose polysaccharide group was 55.11 ± 5.53 pg/mL which was similar to the positive control group (55.92 ± 3.97 pg/mL). The IL-2 level in the medium- and high-dose polysaccharide groups were respectively 82.63 ± 4.05 and 69.27 ± 1.22 pg/mL, which were higher than the normal (60.69 ± 2.56 pg/mL) and the positive control groups. At a dose of 200 mg/kg per day, AMC polysaccharides exhibited the most powerful impact on serum IL-2 level ($P < 0.01$). As described in Figure 3, TNF- α content in the model group was 284.21 ± 28.85 pg/mL and showed significant difference ($P < 0.05$) compared to the normal group (235.53 ± 6.50 pg/mL). AMC polysaccharides presented stronger inhibitory activity towards TNF- α than vitamin E. TNF- α content in the low- and medium-dose polysaccharide groups were respectively 240.79 ± 20.07 pg/mL and 238.16 ± 9.30 pg/mL which were approximate to the high-dose polysaccharide group (244.74 ± 18.64 pg/mL). Regardless of the tremendous mouse-to-mouse variabilities in response to AMC polysaccharides and the lack of statistical significance in some of the observed trends, these data demonstrated that the aging changes mentioned above were reversed by AMC polysaccharides.

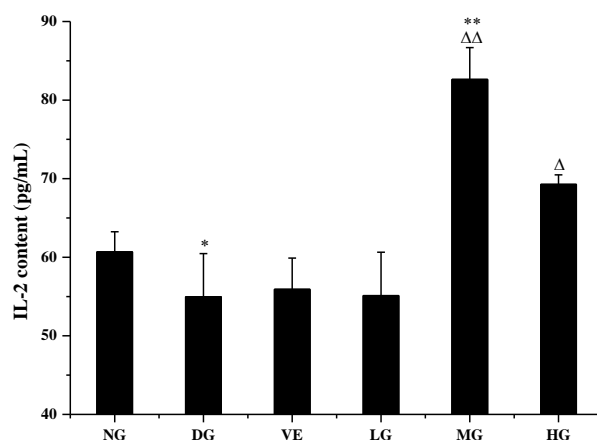


Figure 2. Effect of AMC polysaccharides on IL-2 content in mouse serum (n = 8). * $P < 0.05$, ** $P < 0.01$, compared with the normal group (NG). ^Δ $P < 0.05$, ^{ΔΔ} $P < 0.01$, compared with the model group (DG)

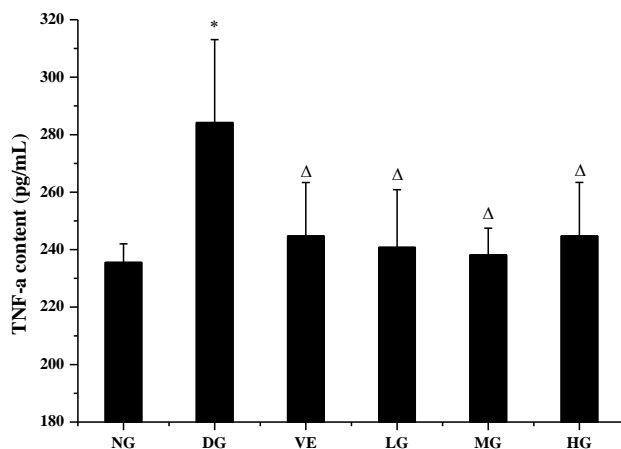
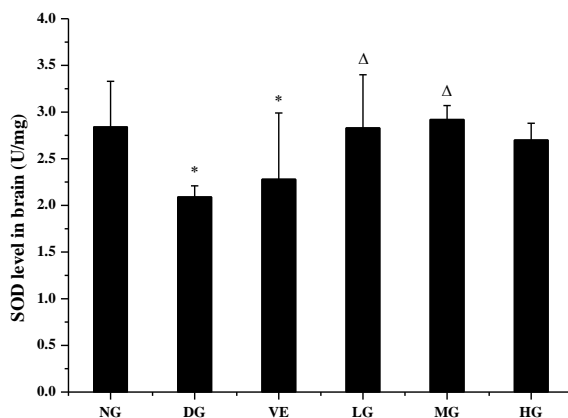


Figure 3. Effect of AMC polysaccharides on TNF- α content in mouse serum (n = 6). * P<0.05, compared with the normal group (NG). Δ P<0.05, compared with the model group (DG)

Effect of AMC Polysaccharides on SOD and CAT Activities

The activities of SOD in mouse brain and liver were represented in Figure 4. As depicted in the figures, AMC polysaccharides significantly enhanced SOD activities. In the brain tissue, SOD activity in the polysaccharide groups were stronger than the positive control group. The medium-dose polysaccharide group emerged the strongest SOD activity of 2.92 ± 0.15 U/mg with a statistically significant difference (P<0.05) compared with the model group. In the liver tissue, the low-dose polysaccharide group showed the highest SOD activity of 27.96 ± 0.02 U/g, which was higher than the normal (20.61 ± 0.05 U/g) and positive control (23.35 ± 0.08 U/g) groups. Apparently, SOD level in the brain tissue was higher than that in the liver tissue.



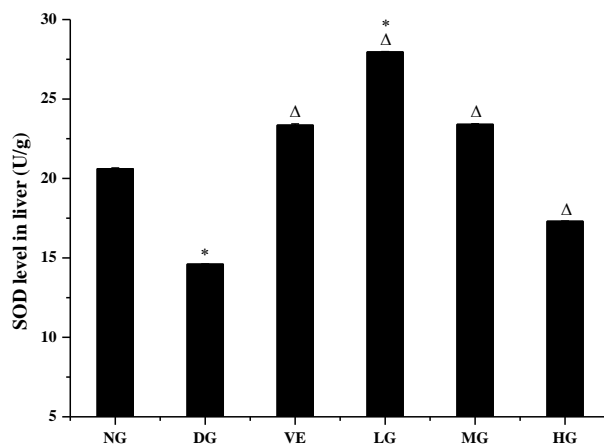
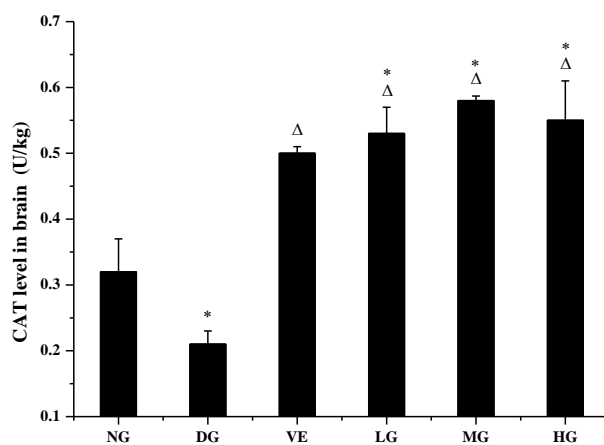


Figure 4. Effect of AMC polysaccharides on SOD activities in mouse brain and liver (n = 6). * $P < 0.05$, compared with the normal group (NG). Δ $P < 0.05$, compared with the model group (DG)

The CAT activities in mouse brain and liver were displayed in Figure 5. CAT levels in D-gal-treated mice were decreased, but increased after administration with vitamin E and polysaccharides. In the brain tissue, there was a significant difference ($P < 0.05$) in CAT activity between the model (0.21 ± 0.02 U/kg) and the normal (0.32 ± 0.05 U/kg) groups. The CAT activities in the low-dose (0.53 ± 0.04 U/kg), medium-dose (0.58 ± 0.007 U/kg) and high-dose (0.55 ± 0.06 U/kg) groups were higher than the positive control group (0.50 ± 0.01 U/kg), which had significant differences ($P < 0.05$) contrasted with the normal and model groups. However, CAT activity was lower in the brain tissue than the liver tissue. In the liver tissue, the activity of CAT in the model group was lowered to 0.11 ± 0.02 U/ μ g with a significant difference of $P < 0.05$. In the polysaccharide groups, the CAT levels were respectively 0.16 ± 0.01 , 0.19 ± 0.03 and 0.13 ± 0.01 U/ μ g. CAT level in the medium-dose group was a bit stronger than the positive control group (0.18 ± 0.03 U/ μ g). However, the dose-response relationship was not observed.



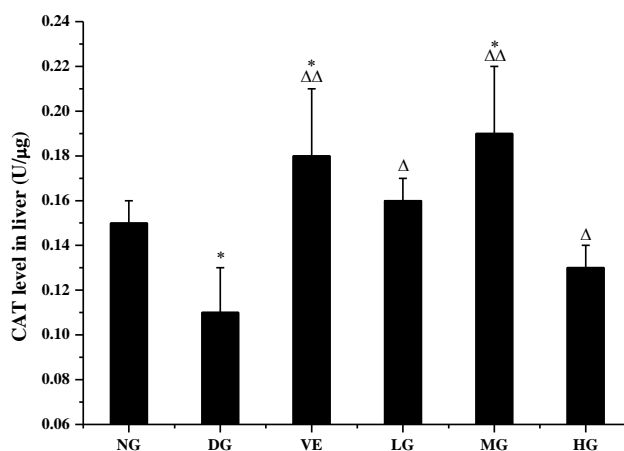


Figure 5. Effect of AMC polysaccharides on CAT activities in mouse brain and liver (n = 6). * $P < 0.05$, compared with the normal group (NG); $\Delta P < 0.05$, $\Delta\Delta P < 0.01$, compared with the model group (DG)

Effect of AMC Polysaccharides on MDA Content

As depicted in Figure 6, AMC polysaccharides minimized MDA content in the liver tissue. In the model group, the MDA content was 1.79 ± 0.05 U/μg and had significant difference of $P < 0.05$ compared with the normal group (1.05 ± 0.02 U/μg). The medium-dose group showed the strongest inhibition effect on MDA (0.74 ± 0.03 U/μg). MDA content in the high-dose group was 0.76 ± 0.01 U/μg, which was close to the medium-dose group and lower than the low-dose group (0.96 ± 0.02 U/μg). MDA content in the brain was determined in this experiment, but showed no significant difference.

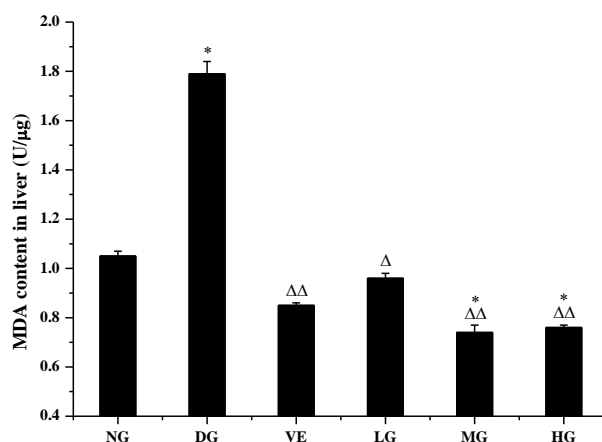


Figure 6. Effect of AMC polysaccharides on MDA content in mouse liver (n = 6). * $P < 0.05$, compared with the normal group (NG); $\Delta P < 0.05$, $\Delta\Delta P < 0.01$, compared with the model group (DG)

Effect of AMC polysaccharides on expression of p53, p21 and SIRT1 genes

The roles of SIRT1, p53 and p21 genes in the anti-aging effect of AMC polysaccharides were investigated and the mRNA expression levels were displayed in Figures 7-9. According to Figures 7 and 8, high gene expression of p53 and p21 occurred in the model group. p53 and p21 levels were respectively decreased to 0.11 ± 0.009 ($P < 0.01$) and

0.55 ± 0.03 ($P < 0.01$) after treated with AMC polysaccharides at 100 mg/kg per day for 50 days. The expression levels of p53 and p21 in the positive control group were 0.74 ± 0.013 and 1.31 ± 0.06 , which were higher than the low-dose polysaccharide group. However, AMC polysaccharides exhibited weak regulation capacity towards p53 and p21 at 200 (3.47 ± 0.05 , 3.68 ± 0.02) and 400 (3.82 ± 0.03 , 4.55 ± 0.04) mg/kg. Obviously, AMC polysaccharides diminished the expression levels of p53 and p21 at the low dose.

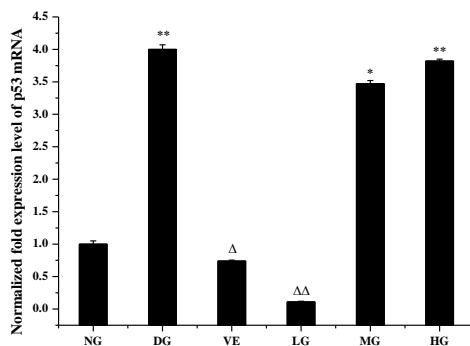


Figure 7. Effect of AMC polysaccharides on p53 gene expression in mouse liver (n = 6). * $P < 0.05$, ** $P < 0.01$, compared with the normal group (NG). Δ $P < 0.05$, ΔΔ $P < 0.01$, compared with the model group (DG)

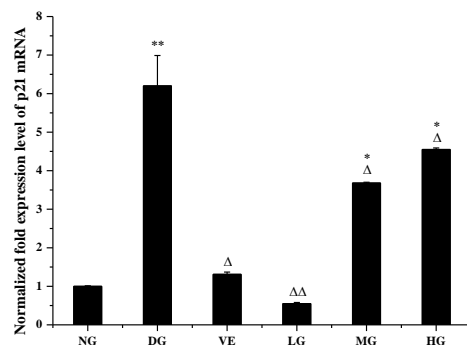


Figure 8. Effect of AMC polysaccharides on p21 gene expression in mouse liver (n = 6). * $P < 0.05$, ** $P < 0.01$, compared with the normal group (NG). Δ $P < 0.05$, ΔΔ $P < 0.01$, compared with the model group (DG)

SIRT1 gene expression level was described in Figure 9. At doses of 200 and 400 mg/kg per day, SIRT1 levels were respectively 0.36 ± 0.006 and 0.17 ± 0.007 , which were higher than the model group (0.16 ± 0.005). At the dose of 200 mg/kg, the polysaccharides showed more powerful up-regulating activity on SIRT1 gene than vitamin E.

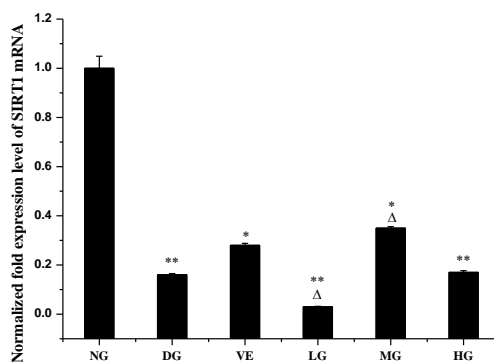


Figure 9. Effect of AMC polysaccharides on SIRT1 gene expression in mouse liver (n = 6). * P<0.05, ** P<0.01, compared with the normal group (NG). Δ P<0.05, compared with the model group (DG)

Effect of AMC polysaccharides on expression of p53 protein

As displayed in Figure 10, p53 protein expression level in the normal group was 0.49 ± 0.001 . After treated with D-gal for 50 days, the protein level raised to 0.70 ± 0.002 and showed a significant difference at $P<0.05$ level compared with the normal group. AMC polysaccharides decreased the level of p53 protein to 0.05 ± 0.002 at 100 mg/kg, but the dose-effect relationship was not appeared. These results illustrated that AMC polysaccharides could simultaneously down-regulate the expression levels of p53 gene and protein. However, the regulation effects of AMC polysaccharides on SIRT1 and p21 proteins were not notable. In spite of the abnormality, SIRT1-p53-p21 pathway was associated with the anti-aging mechanism of AMC polysaccharides.

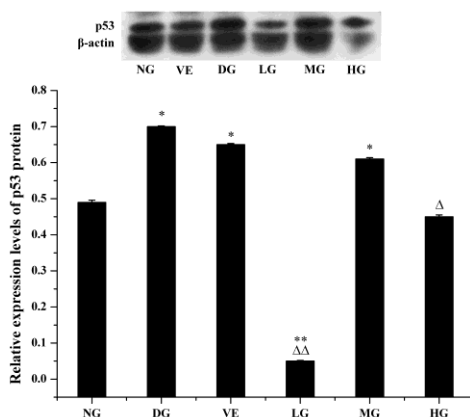


Figure 10. Effect of AMC polysaccharides on p53 protein expression in mouse liver (n = 6). * P<0.05, ** P<0.01, compared with the normal group (NG). Δ P<0.05, ΔΔ P<0.01, compared with the model group (DG)

D-gal induced mouse aging model has been proved exceptionally useful in pharmacological studies for the possible mechanisms of caducity. Numerous researches have confirmed that surplus D-gal can produce excessive free radicals and lipid peroxidation product, and decrease the activity of the antioxidant enzymes which may compensatorily increase the level of carbonyl aldehydes and trigger cellular senescence. Mouse hippocampal slice was often used to confirm the aging in D-gal induced mouse. Hippocampus behaves as a vital brain structure for studies and memories. CA and dentate gyrus (DG) consist the main functional regions of hippocampus and play

important roles in study, memory and visceral functions. CA consists of several cornu ammonis subfields, including CA1, CA2 and CA3. They enable the detection of the early volumetric changes in dementia and neuropsychiatric diseases such as Parkinson's disease, epilepsy and Alzheimer's disease due to their precise pavement and sensitivity towards hypoxia injury [12]. Our results suggested that cells in CA1 area were marked ameliorated after intervention with AMC polysaccharides. We conjectured that higher content of glucose in AMC polysaccharides contributed to the repairment of the damaged hippocampal cells because glucose is the only energy source of the brain tissue [3]. Therefore, the polysaccharides might have beneficial effects on prevention or treatment of the neurodegenerative changes following the oxidative stress evoked in brain areas.

Age-associated decline in protective and immune regulatory functions may result in an increased susceptibility to infections [13]. In our studies, AMC polysaccharides exhibited significant immune regulatory activity by abating TNF- α content, increasing IL-2 level, and increasing the spleen index in D-gal-treated mice. Furthermore, MDA content in the liver was attenuated by the polysaccharides. Taken together, the augmentation of the immune function and the inhibition of the lipid peroxidation reaction might be included in the anti-aging mechanisms of AMC polysaccharides. Early reports revealed that AMC polysaccharides had powerful reducing power, chelating ability and scavenging capacity on superoxide/hydroxyl radicals [14] due to its polyhydroxyl structure and large size, which meant AMC polysaccharides had strong antioxidant activity. Antioxidants may protect against oxidative stress and postpone senescence by means of directly scavenging free radicals or increasing the activities of antioxidant enzymes, including SOD, CAT and GSH-Px [15,16]. Exopolysaccharides from *Agaricus brasiliensis* possessed significant antioxidant capacity and showed eminent anti-aging effect [17]. Therefore, the anti-aging mechanism of AMC polysaccharides was intimately related with their antioxidative actions of augmenting antioxidant enzyme activity and scavenging free radicals.

Senescence is closely related with cancer because both are induced by accumulated oxidative damage. It is approbatory that cellular senescence is mediated by p53/p21 dependent pathway which generally acts as tumor suppressor and biomarker of aging [18,19]. Hence, senescence is closely related with the regulation of p53/p21 pathway. Findings from Chen et al. revealed that p53 and p21 were involved in the hepatic stellate cells senescence triggered by *Schistosoma japonicum* egg antigen p40 (Sjp40) and the silencing of p53 could reverse Sjp40-induced senescence in LX-2 cells [20]. Zhou et al. reported that p53/p21 pathway played an important role in the senescence of cartilage end plates (CEP) cells in vivo/in vitro, SIRT1 alleviated the oxidative stress-induced senescence of CEP cells in humans via p53/p21 pathway [21]. In our study, AMC polysaccharides down-regulated the expression levels of p53/p21 genes and p53 protein, and up-regulated SIRT1 gene expression, which provided a good explanation for their anti-aging actions. These results testified our previous assumptions of the relationships between AMC polysaccharides and SIRT1/p53/p21 pathway.

A retrospective analysis of the available data indicated that high-dose of AMC polysaccharides (400 mg/kg) presented weaker anti-aging activity than low- and medium-dose of polysaccharides (100, 200 mg/kg). It signified that AMC polysaccharides might appear adverse effect on mouse at 400 mg/kg. We supposed that might be due to the monosaccharide component of galactose in AMC polysaccharides. It is well known that polysaccharides can be

partially converted into monosaccharides in the organisms, so higher dosage of AMC polysaccharides implied higher content of the galactose, which might provoke synergy effect with D-gal in mouse. Hence, a high-dose of AMC polysaccharides intaking (≥ 400 mg/kg per day) might be adverse.

CONCLUSION

In a word, current findings provided us new insights into the anti-aging mechanisms of AMC polysaccharides. AMC polysaccharides might possess beneficial effects on preventing aging-associated diseases and the adjuvant therapy for cancer. AMC might be a good source for the anti-aging drugs.

ACKNOWLEDGMENTS

This work was supported by the National Natural Science Funds of China (No. 81774125 & 81573717), the Natural Science Foundation of Shandong province (No. ZR2018LH017), the Project of Shandong Province Higher Educational Science and Technology Program (No. J16LM04, J17KB097, J16LM11 & J15LL54) and Traditional Chinese Medicine Science and Technology Development Project of Shandong Province (No. 2017-205 & 2015-237).

REFERENCES

- [1] DM Liu; JW Sheng; SH Wang; WF Zhang; XH Zhang; DY Wang; *Chin J Experim Trad Med Formul.* **2016**, 22, 59-62.
- [2] DM Liu; JW Sheng; SH Wang; WF Zhang; W Zhang; DJ Zhang. *Molecules.* **2016**, 21, 1280.
- [3] DM Liu; JW Sheng; ZJ Li; HM Qi; YL Sun; Y Duan; WF Zhang. *Int J Biol Macromol.* **2013**, 56, 1-5.
- [4] DM Liu; JW Sheng; HM Qi; WF Zhang. *J Chem Pharm Res.* **2015**, 7, 386-389.
- [5] JW Sheng; YL Sun. *Carbohydr Polym.* **2014**, 108, 41-45.
- [6] D Harman. *Biogerontol.* **2009**, 10, 783.
- [7] PD Adams. *Mol Cell.* **2009**, 36, 2-14.
- [8] A Borodkina; A Shatrova; P Abushik; N Nikolsky; E Burova. *Aging (Albany NY).* **2014**, 6, 481-495.
- [9] MJ Regulski. *Wounds.* **2017**, 6, 168-174.
- [10] EL Zhang; QY Guo; HY Gao; RX Xu; SY Teng; YJ Wu. *Plos One.* **2015**, 10, e0143814.
- [11] VM Doan; C Chen; X Lin; VP Nguyen; Z Nong; W Li; Q Chen; J Ming; Q Xie; R Huang. *Food Funct.* **2015**, 6, 1712-1718.
- [12] D Berron; P Vieweg; A Hochkepler; JB Pluta; SL Ding; A Maass; A Luther; L Xie; SR Das; DA Wolk; T Wolbers; PA Yushkevich; E Düzel; LEM Wisse. *Neuroimage Clin.* **2017**, 15, 466-482.
- [13] H Radbruch; R Mothes; D Bremer; S Seifert; R Köhler; J Pohlan; L Ostendorf; R Gunther; R Leben; W Stenzel; RA Niesner; AE Hauser. *Front Immunol.* **2017**, 8, 844.
- [14] DM Liu; JW Sheng; HM Qi; WF Zhang; CM Han; XL Xin. *J Med Plants Res.* **2011**, 5, 3061-3066.
- [15] SB Izabela; B Grzegorz. *Biomed Res Int.* **2014**, 404680.
- [16] JM Lu; PH Lin; QZ Yao; CY Chen. *J Cell Mol Med.* **2010**, 14, 840-860.
- [17] J Zhang; Z Gao; S Li; S Gao; Z Ren; H Jing; L Jia. *Int J Med Mushrooms.* **2016**, 18, 1071-1081.
- [18] CM Beauséjour; A Krtolica; F Galimi; M Narita; SW Lowe; P Yaswen; J Campisi. *EMBO J.* **2003**, 22, 4212-4122.
- [19] J Campisi. *Annu Rev Physiol.* **2013**, 75, 685-705.
- [20] J Chen; T Xu; D Zhu; J Wang; C Huang; L Lyu; B Hu; W Sun; Y Duan. *Cell Death Dis.* **2016**, 7, e2315.
- [21] N Zhou; X Lin; W Dong; W Huang; W Jiang; L Lin; Q Qiu; X Zhang; J Shen; Z Song; X Liang; J Hao; D Wang; Z Hu. *Sci Rep.* **2016**, 6, 22628.